Aspects of the Tempering Transformation Kinetics of Cr Low Alloyed Steels

A. Munteanu and D. Munteanu

Faculty of Materials Science and Engineering
"Transilvania" University of Brasov – Romania

(Received June 22, 1999; final form August 10, 1999)

ABSTRACT

The paper analyses the kinetics of the carbide coherence loss and carbide coalescence taking place during tempering of low-alloy steels without molybdenum. For complete and incomplete hardening, the thermo-kinetics parameters of coalescence, the values of the reaction constants and the experimental activation energy values have been calculated.

These results have shown that the tempering kinetics for the first stage of tempering (the coherence loss) is different from that for the second stage of tempering (the carbide coalescence), respectively.

1. INTRODUCTION

From a kinetics point of view, it is very difficult to analyze the transformations that appear during tempering between 400 – 600°C, in the case of low–alloy steels. In particular, analysis of the coalescence phenomenon of the "ε-enriched carbon" phases and the coherence loss from the global ferritic matrix is complicated. The paper analyses the two phenomena in separate modes for two kinds of hardening: a "complete hardening", which occurs at temperatures exceeding A_3 and an "incomplete hardening" which occurs at temperatures between A_1 and A_3 The incomplete hardening has been proven to be very effective avoiding the tempering fragility phenomenon of the low-alloy steels.

The carbide coalescence phenomenon during tempering, which appears after the ferritic recrystallization and coherence loss, consists of a gradual disappearance of small particles and growth of the large particles. The transformation force is represented by a change in the free energy of the system (ferrite + carbides) at a constant temperature. This process is realised by a decrease of the total area of the interface between ferrite and carbides.

The tempering coalescence is a consequence of carbon dissolution, carbon diffusion and carbon precipitation phenomena. It is supposed that the carbides tend to be gradually dissolved in ferrite; thus, the carbon concentration in the ferrite becomes high. When the system contains carbides of different sizes, there appears between the nearest zones of the big carbides a carbon concentration gradient of ferrite. The concentration gradient can induce the carbon diffusion towards the large carbides, and finally they grow.

At a constant temperature, the free energy variation corresponding to the carbon transfer is equal to a change in interfacial energy.

1. THEORETICAL ASPECTS ON THE PROCESSES KINETICS

The kinetics of some complex processes such us dissolution, diffusion, precipitation which depends on the temperature, the chemical composition and the dislocation density of the ferritic matrix, is very hard to describe by an analytical equation. Thus, in some cases, when the transformation takes place at a constant temperature, the kinetics parameters are estimated in an

experimental way. The transformation rate could be expressed by the following equation:

$$-\frac{dP}{dt} = K^n t^{n-1}(P-C) \qquad (1)$$

where:
P is the analyzed parameter which is a variable during the isotherm transformation process;
C is the parameter value for the equilibrium conditions;
t is the time of the process;
K,n are constants of the transformation process.

Since a direct proportional relation exists between the variation of some physico-mechanical properties and the proceeding transformation process, we chose the hardness /1/. The "P" parameter characterizes the carbides coalescence.

As Equation (1) is integrated under boundary conditions (the parameter P representing the hardness value, changes from the initial value P_0 to the final value C), $P_{(t)}$ is given by:

$$P_{(t)} = (P_0 - C)e^{-(kt)^n} + C \qquad (2)$$

where k=K/n.

If H_t, H_f and H_0 are the momentary hardness, the final hardness in equilibrium and the initial hardness respectively, Equation (2) becomes /2/:

$$W = \frac{H_t - H_f}{H_0 - H_f} = e^{-(kt)^n} \qquad (3)$$

Equation (3) presents the "structural fraction" <w> not affected by the coalescence phenomenon. This equation represents a typical Johnson-Mehl equation that characterizes the global kinetics of non-homogeneous transformation:

$$y = 1 - e^{-(kt)^n} \qquad (4)$$

where <y> is the variation of the structural fraction with time (which in this case is affected by the coalescence phenomenon). <y> takes values between 0 and 1, corresponding to <w> in Equation (3).

In other words, w=1-y and thus, the <y> expression becomes /3,4/:

$$y = \frac{H_0 - H_t}{H_0 - H_f} = 1 - e^{-(kt)^n} \qquad (5)$$

In order to estimate the kinetics parameters, **k** and **n**, Equation (3) is expressed in a logarithmic form, as follows:

$$\log(-\log W) = n\cdot\log t + n\cdot\log k + \log(\log e) \qquad (6)$$

where: <log t> and <log(-log w)> are the straight-line coordinates and <w> is obtained by means of the hardness measurements.

The <n> parameter represents the line-slope in this plot. For example, this value can be estimated if two points (experimentally established) for the moments t_1 and t_2 are known:

$$n = \frac{\log\left(\log\frac{W_1}{W_2}\right)}{\log\frac{t_1}{t_2}} \qquad (7)$$

Following calculation of the <n> parameter, the "transformation-rate constant <k>" for the coalescence process can be obtained:

$$k = \frac{1}{t_1}\sqrt[n]{\frac{-\log W_1}{\log e}} \qquad (8)$$

With more than two experimental points of <log(-log w)> and <log t>, the equation of linear function (6) is obtained by regression. Thus, the <n> parameter can be estimated from the line-slope, and the <k> parameter corresponds to the distance of the Oy-origin point determined by intersection of the regression-line and the Oy-axis /5/.

In most transformation cases, which take place at a constant temperature, the coefficient of transformation rate <k> depends on three main parameters: the activation energy, the temperature and the frequency factor. These parameters are contained in the Arrhenius equation:

$$k = A \cdot e^{-\frac{Q_A}{RT}} \quad (9)$$

The activation energy Q_A and the frequency factor A characterize an individual phenomenon which takes place during the coalescence process. The value of <k> could be considered an individual constant of microscopic phenomena. Thus, the method leads to the average values of Q_A and A in the case of coalescence. Therefore, a logarithmic form of the Arrhenius equation can be employed:

$$\log k = \frac{Q_A}{R} \cdot \log e \cdot \frac{1}{T} + \log A \quad (10)$$

If Q_A and A are constant values, the curve of log k versus (1/T) represents a straight line. The slope of this straight line, <m>, gives an activation energy Q_A=(mR/log e), and the intersection between this straight line and the <log k> axis make it possible to obtain the frequency factor A.

3. EXPERIMENTAL RESULTS

The coalescence kinetics parameters have been obtained in a low-alloyed steel: 40Cr10 (≅En 19/NS) with the following composition (wt-%): 0,42C; 0,61Mn; 0,35Si; 1,03Cr. First of all, the A_{c1} and A_{c3} points were determined via the differential dilatability method – Chevernard type. In this experiment, some typical annealed samples (ϕ 4,4 x 65,1 mm) were used.

The A_1 and A_3 temperatures in this steel were 760°C and 830°C. The hardening temperatures for the complete hardening and for the incomplete hardening were estimated to be 860°C and 790°C, respectively.

Following complete hardening, the hardness value was 57±1 HRC and the microstructure was a total martensitic structure, without residual austenite. After the incomplete hardening, the hardness value was 45±1 HRC for the ferritic microstructure which did not turn into austenite on heating and then into martensite on quenching.

The critical heating temperature, at which the carbide coalescence loss from the ferritic matrix appeared, was established graphically by measuring the dilatability of hardened samples. Thus, for the incompletely hardened sample, the temperature was 445°C, and 475°C for the completely hardened sample, as shown in Fig. 1. These temperatures are noted on the dilatability curve by the change in slope.

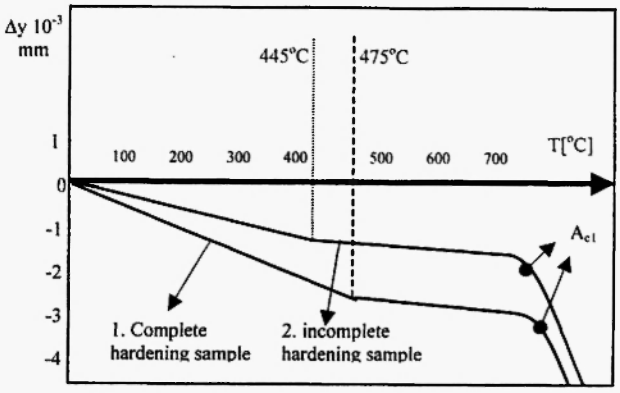

Fig. 1: Dilatability curves typical of the hardened samples (differential dilatability method – Chevenard type).

In order to estimate the critical hardness value typical of the coherence loss phenomenon, experimental samples (by fives ϕ 10 X 10 mm) of the steel (40Cr10) were manufactured. They were oil-quenched from 860°C and 790°C.

Then, the samples were tempered in a salt bath at 445°C and 475°C for 75 minutes. The hardening temperatures were suited to the carbides coherence loss.

The maintaining times were obtained from the dilatability curves (Fig. 1) by planimetry considering the heating rate of the Chevenard dilatability device. In order to estimate the period which produces a dilatability under more rapid heating conditions (in a salt-bath, S 220 type) than the heating conditions of dilatability device, the following relation was used:

$$t_{heating} = \frac{1}{\Delta l_f} \int_0^{t_1} l(t)dt \quad (11)$$

where:

Δl_f is the dilatability value for coherence loss;

t_1- the time at which the coherence loss appears for a constant heating rate (3°C/min.- heating in the dilatability device).

Observation of the tempered samples by scanning

Table 1

Coalescence process estimation for complete hardening, via hardness analysis

Temperature [°C]	Time, t [min.]	log t	H_0	H_t	W, [%]	log(-logW)	n	K, [1/min.]
			HV					
500	15	1,17609	420	400	71,42	-0,83656	0,89	0,0179
	30	1,47712		390	57,14	-0,61432		
	45	1,65321		385	50	-0,52139		
	60	1,77815		369	27,14	-0,24692		
	120	2,07918		350	0			
550	15	1,17609	420	349	43,2	-0,43828	0,40	0,0415
	30	1,47712		336	32,8	-0,31504		
	45	1,65321		328	26,4	-0,23777		
	60	1,77815		323	23,2	-0,19756		
	120	2,07918		295	0			
600	15	1,17609	420	317	28,96	-0,26912	0,46	0,1029
	30	1,47712		302	18,62	-0,13667		
	45	1,65321		293	12,41	-0,04283		
	60	1,77815		289	9,65	-0,00657		
	120	2,07918		275	0			

Table 2

Coalescence process estimation for incomplete hardening, via hardness analysis

Temperature [°C]	Time, t [min.]	log t	H_0	H_t	W, [%]	log(-logW)	n	K, [1/min.]
			HV					
500	15	1,17609	330	310	71,42	-0,83656	0,71	0,015
	30	1,47712		297	52,85	-0,55768		
	45	1,65321		293	47,14	-0,48600		
	60	1,77815		288	40	-0,40018		
	120	2,07918		260	0			
550	15	1,17609	330	269	23,75	-0,20458	0,44	0,129
	30	1,47712		266	20	-0,15554		
	45	1,65321		261	13,75	-0,06464		
	60	1,77815		255	6,25	-0,08067		
	120	2,07918		250	0			
600	15	1,17609	330	261	23,33	-0,19926	0,35	0,165
	30	1,47712		257	18,88	-0,14038		
	45	1,65321		252	13,33	-0,05796		
	60	1,77815		248	8,88	0,02166		
	120	2,07918		240	0			

electron microscopy confirms that little carbides exist in the microstructure, which indicate that they are homogeneously distributed. In Tables 1 and 2, the average hardness values measured after tempering are given. The hardness values of completely hardened samples and incompletely hardened samples are 420 HV and 330 HV, respectively. These values are denoted H_0, which indicates the coherence loss of the carbides.

Then, samples (ϕ10 x 10 mm) were hardened via oil quenching and tempered in the salt bath, in accordance with data shown in Tables 1 and 2. By tempering the hardness was changed and the average values of three samples were recorded in the tables.

Further, the kinetics parameters were calculated using the method described above; the hardness value H_f from Equation (3) was obtained after annealing for two hours. In order to estimate the constant values <n> and <k>, the experimental points are plotted and the regression lines are drawn in Fig. 2 and 3 /5,6/. Figs. 2 and 3 show the experimental points on the right-line for each hardening condition and tempering temperature. The coalescence kinetics for the two hardening conditions can be described by means of some equations (S-type) for any temperature between 500-600°C, considering an average value of the <n> coefficient. This value is almost constant when the analyzed phenomenon represents a common proceeding mechanism:

- *for complete hardening*
  $T_{tempering} = 550°C$

$$\frac{H_t - H_f}{H_0 - H_f} = e^{-(0{,}0415\,t)^{0.40}} \qquad (12)$$

- *for incomplete hardening*
  $T_{tempering} = 550°C$

$$\frac{H_t - H_f}{H_0 - H_f} = e^{-(0{,}129\,t)^{0.34}} \qquad (13)$$

In fact, the <n> coefficient value calculated for T=500°C is different from those for the temperatures T=550°C and T=600°C (see Tables 1 and 2). This means that the coalescence mechanism depends on the

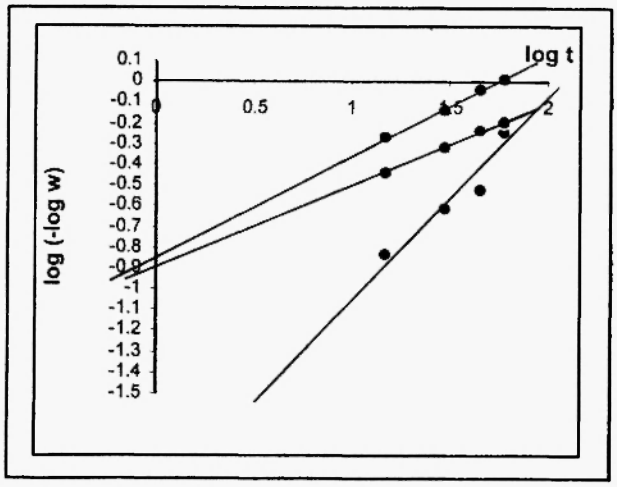

Fig. 2: The regression straights of the transformation process for different constant temperatures after complete hardening.

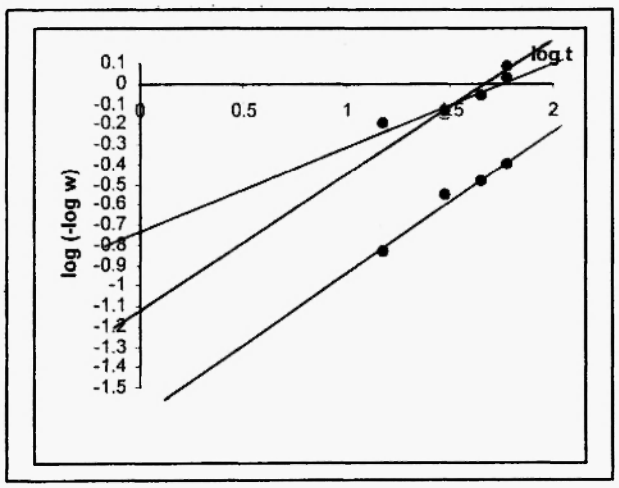

Fig. 3: The regression straights of the transformation process for different constant temperatures after incomplete hardening.

tempering temperature. The aspect is also observed in the value of the reaction rate coefficient <k>.

The activation average energies were estimated from the reaction rate constant values for three temperatures, coupled with the Arrhenius equation, as shown in Tables 3 and 4. The reaction rates of coalescence processes for tempering between 500°C and 600°C are described as follows:

- *for complete hardening*
  $T_{tempering} = 550^{o}C$

$$k = 6{,}66 \cdot 10^{4} \cdot e^{\frac{23195}{RT}} \ [1/\min]. \quad (14)$$

- *for incomplete hardening*
  $T_{tempering} = 550^{o}C$

$$k = 2{,}97 \cdot 10^{7} \cdot e^{\frac{32335}{RT}} \ [1/\min]. \quad (15)$$

where: R=1,98 cal./mol K (the gas constant) and T is the isothermal annealing temperature [K] /7/.

4. CONCLUSIONS

The microstructure of incomplete hardening, which consists of martensite and a ferrite mixture, shows a special global kinetics during tempering, which is different from the case of the total martensitic structure.

Loss of carbide coherence distinguished by a change in the slope of the dilatability curve takes place at 445°C, which is lower than the complete hardening case, 475°C. Thus, in the case of incomplete hardening, the presence of ferrite and martensite in unstable equilibrium conditions, in which martensite contains a relatively higher carbon concentration, leads to carbon separation for lower temperatures.

When the coherence has been lost, the kinetics of coalescence processes of complete hardening shows a transformation rate higher than that of incomplete hardening. This conclusion can be proven by a relatively lower value of the <n> coefficient (see Table 2) and a higher value of coalescence activation energy, for the incomplete hardening.

The above aspects can be explained by the average free energy variation of the thermodynamic system configuration (see Fig. 4) during tempering, for the two hardening conditions.

The martensitic structure, which is obtained after complete hardening, shows a free energy value higher than that of martensitic-ferrite structure obtained after the incomplete hardening.

Both microstructures reveal free energy values higher than the energy equilibrium value of the final state (the equilibrium final state is characterized by a ferritic global structure and small carbides). The outrunning of the transient state (therefore, the activation of iron and carbon atoms) may be described by an energy consumption Q_A with the transformation force ΔF (see Fig.4).

For complete hardening, the calculated value of

Table 3

Estimation of the frequency factor and the activation average energy for complete hardening

Temperature, [K]	k, [1/min.]	log k	1/T 10^3	Q_A, [cal./mol]	A, [1/min.]
773	0,0179	-1,74715	1,294	23195	66690
823	0,0415	-1,38195	1,215		
873	0,1029	-0,98758	1,145		

Table 4

Estimation of the frequency factor and the activation average energy for incomplete hardening

Temperature, [K]	k, [1/min.]	log k	1/T 10^3	Q_A, [cal./mol]	A, [1/min.]
773	0,015	-1,82391	1,294	32335	2,97 10^7
823	0,129	-0,88941	1,215		
873	0,165	-0,78251	1,145		

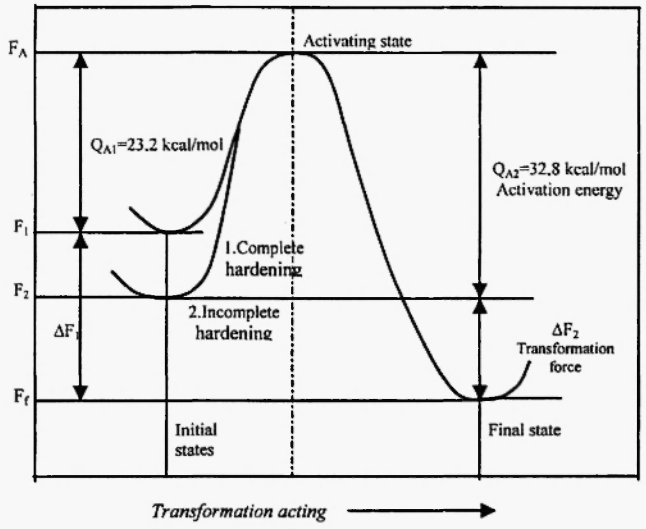

Fig. 4: The variation of average free energy during tempering.

activation energy for coalescence (beginning from 475°C), 23,2 kcal/mol, does not include a calculation error. The activation energy during tempering (≅ 57 kcal/mol), which intervenes in the tempering parameter estimation, has been established until now for temperature values between 400°C and A_{c1}, in /8/, for an initial martensitic structure. The difference in the activation energy is considered to be due to the state of coherence loss as an initial state /8/. In these conditions, the difference value of 35,2 kcal/mol represents the activation energy of the ε-phase forming and coherence loss and the activation energy of ferrite recrystallization.

The value of coalescence activation energy obtained in the complete hardening case is nearly equal to the activation energy for carbon diffusion (carbon diffusion in ferrite). For temperatures between 500°C and 600°C, this parameter value is 18,5 kcal/mol. This means that the coalescence phenomenon is based on carbon diffusion.

REFERENCES

1. J. Burke, *La cinetique des changements de phase dans les metaux*, Ed. Masson, Paris (1968).
2. P.D. Anderson, R. Hultgren, *The thermodynamics of solid iron at elevated temperatures*, Trans. AIME, vol. 224, 882 (1968).
3. A. Munteanu, *Teoria transformarilor de faza in stare solida*, Brasov, 1995.
4. G.R. Speich, *Tempering of low carbon martensite*, Trans. AIME, vol. 245, 2253, (1969).
5. R.A. Grange, Hardness of tempered martensite in carbon and low-alloy steels, Metallurgical Trans., A., vol. 8A, 1775, (1977).
6. C.L. Briant, *Role of carbides in tempered martensite embrittlement*, Materials Science and Technology, 2, 138,(1985).
7. A. Munteanu, *Considerations sur la cinetique des processus de graphitisation des fontes GS perlitiques*, ATTT- Gand, (1993).
8. A. Constant, G. Henry, J.C. Charbounier, *Principe de base des traitements thermique des aciers*, PYC Edition (1992).